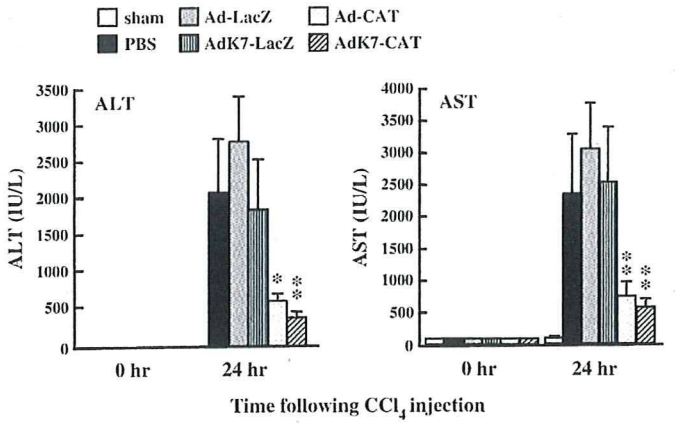

Fig. 6. Preventive effect of catalase-expressing Ad vectors on CCl_4-induced acute liver failure. CCl_4 (1 ml/kg) was intraperitoneally injected to mice 48 h following Ad vector injection. Serum samples were collected 24 h after CCl_4 administration. The data are expressed as the means ± S.D. ($n = 4$). *Significantly different from the PBS-injected group at $p<0.05$; ** at $p<0.01$.

3.5. Improvement of survival rates of mice subjected to partial hepatectomy and hepatic ischemia/reperfusion by catalase-expressing Ad vectors

To examine whether over-expression of catalase improves the remnant liver function in mice subjected to both partial hepatectomy and I/R treatment, partial hepatectomy and subsequent I/R treatment were conducted 48 h after pre-administration of Ad vectors. Partial hepatectomy is often performed under hepatic ischemia, and the remaining liver suffers from I/R injury after partial hepatectomy in clinical settings. Mice pre-administered with AdK7-CAT showed a dramatic improvement in survival rate (Fig. 7). Seventy percent of mice survived for 7 days after these treatments. The body weights of the mice pre-injected with AdK7-CAT were not significantly reduced 7 days after surgery, compared with those before surgery (data not shown), suggesting that the general health of the mice was not substantially compromised after the surgery. On the other hand, the survival of the mice was not prolonged by pre-administration of Ad-LacZ or PBS. These results indicate that catalase-expressing Ad vectors are able to protect the liver from more serious stress induced by partial hepatectomy and I/R, and to improve the remnant liver function.

4. Discussion

Hepatotoxins, drugs, and I/R can injure the liver via oxidative stress. With the aim of efficiently preventing oxidative stress-induced hepatic injury, we pre-administered Ad vectors expressing an antioxidative enzyme, catalase, to mice. The results of our study demonstrated that Ad vector-mediated over-expression of catalase in the liver effectively prevents hepatic injury caused by not only I/R but also CCl_4. Furthermore, the survival rates of mice subjected to both partial hepatectomy and I/R treatment were prolonged by over-expression of catalase.

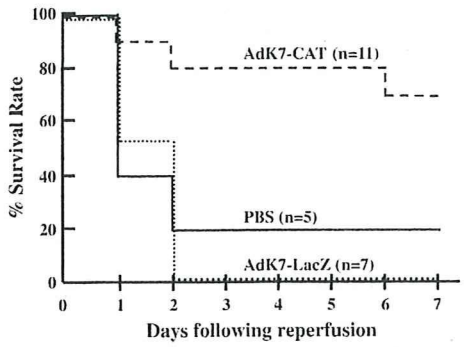

Fig. 7. Survival rates of mice subjected to partial hepatectomy and hepatic I/R following Ad vector administration. Solid line: PBS ($n = 5$); dotted line: AdK7-LacZ ($n = 7$); dashed line: AdK7-CAT ($n = 11$). Ad vectors were intravenously administered to mice as described in Fig. 4. Forty-eight hours after Ad vector administration, mice were subjected to two-thirds partial hepatectomy, followed by an 8 min-period of ischemia

Superoxide anion is the primary oxidant species generated during hepatic I/R by a xanthine oxidase system and/or decoupling of the electron transport system in mitochondria. Superoxide anion is readily converted to H_2O_2 by SOD or a spontaneous reaction. H_2O_2 itself is a weak oxidizing agent; however, hydroxyl radical is produced by H_2O_2 in the presence of transition-metal ion. Hydroxyl radical has the most oxidative ability and the strongest toxicity among the various ROS. Reduction/elimination of hydroxyl radical is considered to be the most effective strategy for prevention of hepatic I/R injury. Therefore, catalase, which prevents generation of hydroxyl radical by converting H_2O_2 to H_2O and O_2, was selected as the antioxidant enzyme in the present study. Catalase derivatives also exhibited higher preventive effects on the elevation of serum ALT and AST levels induced by hepatic I/R, compared with SOD derivatives [5,6]. In addition, over-expression of catalase in the liver might increase endogenous expression of SOD, which is another advantage of catalase gene transfer. He et al. demonstrated that delivery of catalase gene alone to the liver induced SOD activity in the liver [17].

Partial hepatectomy is often performed under hepatic ischemia. Previous studies have shown that oxidative stress induced by hepatic I/R affects hepatocyte cell death and inhibits liver regeneration [42,43]. Beyer et al. reported that ROS are directly responsible for the impairment of insulin/insulin-like growth factor 1 signaling, which is crucial for liver regeneration [44]. Furthermore, hepatocytes without catalase activity have been found in regenerating livers after partial hepatectomy [45], suggesting that hepatocytes in the regenerating livers might be susceptible for ROS-mediated injury. The present study demonstrated that over-expression of catalase in the liver dramatically improved the survival rates of mice subjected to partial hepatectomy and I/R, suggesting that the remnant livers would be protected from ROS-mediated injury by over-expression of catalase. Furthermore, over-expression of catalase might play an important role in maintenance of the regenerative capacity of hepatocytes. Recently, removal of ROS by antioxidant enzymes was demonstrated to be crucial for maintenance of the self-renewal capacity of progenitor/stem cells in an *in vitro* culture system [46,47]. In this study, the liver/body weight ratio of mice pre-injected with AdK7-CAT 1 week after partial hepatectomy and I/R was 4.7 ± 0.55%, which is not significantly different from that of naïve mice (data not shown).

Oxidative stress is also generated in the liver through metabolism of a variety of drugs, chemicals, and toxins, such as thioacetamide, lipopolysaccharide, and CCl_4. In particular, CCl_4 is often used as a representative hepatotoxin causing oxidative stress in animal experiments. CCl_4 is metabolized by cytochrome P450 in the endoplasmic reticulum of hepatocytes, leading to generation of CCl_3 radical, which induces hepatic damages, although the mechanism of CCl_4-mediated liver damage has not yet been fully revealed. The present study showed that Ad vector-mediated over-expression of catalase in the liver also attenuated CCl_4-induced liver injury (Fig. 6). Over-expression of SOD has also been shown to inhibit CCl_4-induced hepatic damages [48]. Hepatic delivery of genes encoding ROS-deleting enzymes is effective in case of hepatic injury induced by oxidative stress-generating hepatotoxins and chemical compounds.

Ad vectors offer various advantages for gene delivery to the liver; however, systemic administration of Ad vectors often induces inflammatory cytokine production and hepatic damage [24,49–51]. However, we found no apparent Ad vector-induced damages in the liver in this study (data not shown). Moreover, mice pre-administered Ad-LacZ or AdK7-LacZ did not exhibit higher levels of serum ALT and AST after I/R than those pre-administered PBS (Fig. 4). This was likely

due to the relatively low dose of Ad vectors (1×10^{10} VP/mouse) used in this study. Higher doses of Ad vectors have often been administered in the studies reporting Ad vector-mediated *in vivo* toxicities [49,51]. We confirmed that more than 90% of hepatocytes were efficiently transduced even at a dose of 1×10^{10} VP/mouse in this study (data not shown). In general, Ad vectors have been considered more toxic than non-viral vectors containing plasmid DNA; however, our group recently revealed that Ad vectors induced smaller amounts of inflammatory cytokines, which are partly involved in Ad vector-induced hepatic toxicity, following intravenous administration into mice, compared with plasmid DNA/cationic liposome complexes, which were used as a representative of non-viral gene delivery vehicle [23]. In both that previous study and our present work, Ad vectors successfully deliver antioxidant genes to the liver with no apparent toxicity, although we should pay attention to the vector doses.

In addition to conventional Ad vectors, fiber-modified AdK7 vectors, which display a poly-lysine motif on the c-terminal of the fiber knob, [24,35,52] were used in this study. AdK7 vectors mediate not only significantly higher transgene expression in the liver but also lower *in vivo* damages than conventional Ad vectors [24]. However, the serum ALT and AST levels of the mice receiving Ad-CAT and AdK7-CAT were not significantly different from those of the controls in this study (Fig. 4), although histological analysis of the liver sections revealed that AdK7-CAT conferred superior protection against I/R injury (Fig. 5), probably because sufficient levels of catalase would be expressed by Ad-CAT at this dose to prevent hepatic I/R-induced increases in serum ALT and AST in this setting. AdK7-CAT might show higher protective effects than conventional Ad vectors under more severe conditions.

In conclusion, the present study demonstrated that Ad vector-mediated catalase expression in the liver significantly improved I/R-induced hepatic injury. These findings suggests that Ad vectors expressing antioxidant enzymes would contribute to the development of strategies aimed at inhibiting hepatic I/R injury. Antioxidant enzyme-expressing Ad vectors are also applicable for the prevention of I/R-induced injury in other organs and oxidative stress-induced damages caused by ROS-generating chemicals. Moreover, their combined use with other antioxidant genes or anti-apoptosis genes could further attenuate oxidative stress-induced injury.

Acknowledgement

We thank Dr. Yuriko Higuchi (Graduate School of Pharmaceutical Sciences, Kyoto University, Kyoto, Japan) for her help in the liver ischemia/reperfusion experiments. We also thank Dr. Kazuo Ohashi (Institute of Advanced Biomedical Engineering and Sciences, Tokyo Women's Medical University, Tokyo, Japan) for his help in the partial hepatectomy experiment. This work was supported by grants from the Ministry of Health, Labour, and Welfare of Japan.

References

[1] R.G. Thurman, et al., Hepatic reperfusion injury following orthotopic liver transplantation in the rat, Transplantation 46 (1988) 502–506.
[2] J.M. McCord, Oxygen-derived free radicals in postischemic tissue injury, N. Engl. J. Med. 312 (1985) 159–163.
[3] M.J. Arthur, et al., Oxygen-derived free radicals promote hepatic injury in the rat, Gastroenterology 89 (1985) 1114–1122.
[4] D.N. Granger, R.J. Korthuis, Physiologic mechanisms of postischemic tissue injury, Annu. Rev. Physiol. 57 (1995) 311–332.
[5] Y. Yabe, et al., Prevention of neutrophil-mediated hepatic ischemia/reperfusion injury by superoxide dismutase and catalase derivatives, J. Pharmacol. Exp. Ther. 298 (2001) 894–899.
[6] Y. Yabe, et al., Targeted delivery and improved therapeutic potential of catalase by chemical modification: combination with superoxide dismutase derivatives, J. Pharmacol. Exp. Ther. 289 (1999) 1176–1184.
[7] S.L. Atalla, L.H. Toledo-Pereyra, G.H. MacKenzie, J.P. Cederna, Influence of oxygen-derived free radical scavengers on ischemic livers, Transplantation 40 (1985) 584–590.
[8] T. Fujita, et al., Therapeutic effects of superoxide dismutase derivatives modified with mono- or polysaccharides on hepatic injury induced by ischemia/reperfusion, Biochem. Biophys. Res. Commun. 189 (1992) 191–196.
[9] P.S. Pyatak, A. Abuchowski, F.F. Davis, Preparation of a polyethylene glycol: superoxide dismutase adduct, and an examination of its blood circulation life and anti-inflammatory activity, Res. Commun. Chem. Pathol. Pharmacol. 29 (1980) 113–127.
[10] J.F. Turrens, J.D. Crapo, B.A. Freeman, Protection against oxygen toxicity by intravenous injection of liposome-entrapped catalase and superoxide dismutase, J. Clin. Invest. 73 (1984) 87–95.
[11] L. Agrawal, et al., Antioxidant enzyme gene delivery to protect from HIV-1 gp120-induced neuronal apoptosis, Gene Ther. 13 (2006) 1645–1656.
[12] P.Y. Benhamou, et al., Adenovirus-mediated catalase gene transfer reduces oxidant stress in human, porcine and rat pancreatic islets, Diabetologia 41 (1998) 1093–1100.
[13] E. Durand, et al., Adenovirus-mediated gene transfer of superoxide dismutase and catalase decreases restenosis after balloon angioplasty, J. Vasc. Res. 42 (2005) 255–265.
[14] F. Sakurai, H. Mizuguchi, T. Yamaguchi, T. Hayakawa, Characterization of in vitro and in vivo gene transfer properties of adenovirus serotype 35 vector, Mol. Ther. 8 (2003) 813–821.
[15] H. Mizuguchi, et al., CAR- or alphav integrin-binding ablated adenovirus vectors, but not fiber-modified vectors containing RGD peptide, do not change the systemic gene transfer properties in mice, Gene Ther. 9 (2002) 769–776.
[16] R. Alemany, D.T. Curiel, CAR-binding ablation does not change biodistribution and toxicity of adenoviral vectors, Gene Ther. 8 (2001) 1347–1353.
[17] S.Q. He, et al., Delivery of antioxidative enzyme genes protects against ischemia/reperfusion-induced liver injury in mice, Liver Transpl. 12 (2006) 1869–1879.
[18] H. Yin, et al., Pretreatment with soluble ST2 reduces warm hepatic ischemia/reperfusion injury, Biochem. Biophys. Res. Commun. 351 (2006) 940–946.
[19] R.S. Sung, L. Qin, J.S. Bromberg, TNFalpha and IFNgamma induced by innate anti-adenoviral immune responses inhibit adenovirus-mediated transgene expression, Mol. Ther. 3 (2001) 757–767.
[20] N. Morral, et al., Immune responses to reporter proteins and high viral dose limit duration of expression with adenoviral vectors: comparison of E2a wild type and E2a deleted vectors, Hum. Gene Ther. 8 (1997) 1275–1286.
[21] S. Li, L. Huang, In vivo gene transfer via intravenous administration of cationic lipid–protamine–DNA (LPD) complexes, Gene Ther. 4 (1997) 891–900.
[22] S. Li, et al., Effect of immune response on gene transfer to the lung via systemic administration of cationic lipidic vectors, Am. J. Physiol. 276 (1999) L796–L804.
[23] H. Sakurai, et al., Comparison of gene expression efficiency and innate immune response induced by Ad vector and lipoplex, J. Control. Release 117 (2007) 430–437.
[24] N. Koizumi, et al., Fiber-modified adenovirus vectors decrease liver toxicity through reduced IL-6 production, J. Immunol. 178 (2007) 1767–1773.
[25] M.D. Wheeler, et al., Comparison of the effect of adenoviral delivery of three superoxide dismutase genes against hepatic ischemia–reperfusion injury, Hum. Gene Ther. 12 (2001) 2167–2177.
[26] S. Kondo, et al., Mannosylated superoxide dismutase inhibits hepatic reperfusion injury in rats, J. Surg. Res. 60 (1996) 36–40.
[27] B. Chen, et al., Delivery of antioxidant enzyme genes protects against ischemia/reperfusion-induced injury to retinal microvasculature, Invest. Ophthalmol. Vis. Sci. 50 (2009) 5587–5595.
[28] H. Mizuguchi, M.A. Kay, Efficient construction of a recombinant adenovirus vector by an improved in vitro ligation method, Hum. Gene Ther. 9 (1998) 2577–2583.
[29] H. Mizuguchi, M.A. Kay, A simple method for constructing E1- and E1/E4-deleted recombinant adenoviral vectors, Hum. Gene Ther. 10 (1999) 2013–2017.
[30] H. Mizuguchi, et al., A simplified system for constructing recombinant adenoviral vectors containing heterologous peptides in the HI loop of their fiber knob, Gene Ther. 8 (2001) 730–735.
[31] M. Mari, J. Bai, A.I. Cederbaum, Adenovirus-mediated overexpression of catalase in the cytosolic or mitochondrial compartment protects against toxicity caused by glutathione depletion in HepG2 cells expressing CYP2E1, J. Pharmacol. Exp. Ther. 301 (2002) 111–118.
[32] J. Bai, A.I. Cederbaum, Adenovirus-mediated overexpression of catalase in the cytosolic or mitochondrial compartment protects against cytochrome P450 2E1-dependent toxicity in HepG2 cells, J. Biol. Chem. 276 (2001) 4315–4321.
[33] F. Sakurai, et al., Optimization of adenovirus serotype 35 vectors for efficient transduction in human hematopoietic progenitors: comparison of promoter activities, Gene Ther. 12 (2005) 1424–1433.
[34] J.V. Maizel Jr., D.O. White, M.D. Scharff, The polypeptides of adenovirus. I. Evidence for multiple protein components in the virion and a comparison of types 2, 7A, and 12, Virology 36 (1968) 115–125.
[35] N. Koizumi, et al., Generation of fiber-modified adenovirus vectors containing heterologous peptides in both the HI loop and C terminus of the fiber knob, J. Gene Med. 5 (2003) 267–276.
[36] A. Tsung, et al., The nuclear factor HMGB1 mediates hepatic injury after murine liver ischemia–reperfusion, J. Exp. Med. 201 (2005) 1135–1143.
[37] M.R. Duranski, et al., Cytoprotective effects of nitrite during in vivo ischemia–reperfusion of the heart and liver, J. Clin. Invest. 115 (2005) 1232–1240.
[38] K. Ohashi, F. Park, M.A. Kay, Role of hepatocyte direct hyperplasia in lentivirus-mediated liver transduction in vivo, Hum. Gene Ther. 13 (2002) 653–663.
[39] K. Ohashi, et al., Liver tissue engineering at extrahepatic sites in mice as a potential new therapy for genetic liver diseases, Hepatology 41 (2005) 132–140.
[40] T.J. Monks, et al., Quinone chemistry and toxicity, Toxicol. Appl. Pharmacol. 112 (1992) 2–16.
[41] H. Thor, et al., The metabolism of menadione (2-methyl-1, 4-naphthoquinone) by isolated hepatocytes. A study of the implications of oxidative stress in intact cells, J. Biol. Chem. 257 (1982) 12419–12425.
[42] N. Fausto, Liver regeneration, J. Hepatol. 32 (2000) 19–31.

3] H. Kamata, et al., Reactive oxygen species promote TNFalpha-induced death and sustained JNK activation by inhibiting MAP kinase phosphatases, Cell 120 (2005) 649–661.
4] T.A. Beyer, et al., Impaired liver regeneration in Nrf2 knockout mice: role of ROS-mediated insulin/IGF-1 resistance, Embo J. 27 (2008) 212–223.
5] I. Oikawa, P.M. Novikoff, Catalase-negative peroxisomes: transient appearance in rat hepatocytes during liver regeneration after partial hepatectomy, Am. J. Pathol. 146 (1995) 673–687.
6] R.C. Meagher, A.J. Salvado, D.G. Wright, An analysis of the multilineage production of human hematopoietic progenitors in long-term bone marrow culture: evidence that reactive oxygen intermediates derived from mature phagocytic cells have a role in limiting progenitor cell self-renewal, Blood 72 (1988) 273–281.
7] R. Gupta, S. Karpatkin, R.S. Basch, Hematopoiesis and stem cell renewal in long-term bone marrow cultures containing catalase, Blood 107 (2006) 1837–1846.
[48] S.K. Venugopal, et al., Lentivirus-mediated superoxide dismutase1 gene delivery protects against oxidative stress-induced liver injury in mice, Liver Int. 27 (2007) 1311–1322.
[49] M. Christ, et al., Modulation of the inflammatory properties and hepatotoxicity of recombinant adenovirus vectors by the viral E4 gene products, Hum. Gene Ther. 11 (2000) 415–427.
[50] A. Lieber, et al., Inhibition of NF-kappaB activation in combination with bcl-2 expression allows for persistence of first-generation adenovirus vectors in the mouse liver, J. Virol. 72 (1998) 9267–9277.
[51] R.S. Everett, et al., Liver toxicities typically induced by first-generation adenoviral vectors can be reduced by use of E1, E2b-deleted adenoviral vectors, Hum. Gene Ther. 14 (2003) 1715–1726.
[52] T.J. Wickham, et al., increased in vitro and in vivo gene transfer by adenovirus vectors containing chimeric fiber proteins, j. virol. 71 (1997) 8221–8229.

Gene Therapy (2009) 16, 297–302

www.nature.com/gt

SHORT COMMUNICATION

Adenovirus serotype 35 vector-mediated transduction following direct administration into organs of nonhuman primates

F Sakurai[1], S-i Nakamura[2,3,7], K Akitomo[1], H Shibata[2], K Terao[2], K Kawabata[1], T Hayakawa[4,5] and H Mizuguchi[1,6]

[1]*Laboratory of Gene Transfer and Regulation, National Institute of Biomedical Innovation, Ibaraki City, Osaka, Japan;* [2]*Tsukuba Primates Research Center, National Institute of Biomedical Innovation, Tsukuba City, Ibaraki, Japan;* [3]*The Corporation for Production and Research of Laboratory Primates, Tsukuba City, Ibaraki, Japan;* [4]*Pharmaceuticals and Medical Devices Agency, Chiyoda-Ku, Tokyo, Japan;* [5]*Pharmaceutical Research and Technology Institute, Kinki University, Osaka, Japan and* [6]*Graduate School of Pharmaceutical Sciences, Osaka University, Suita City, Osaka, Japan*

Adenovirus (Ad) serotype 35 (Ad35) vectors have attracted remarkable attention as alternatives to conventional Ad serotype 5 (Ad5) vectors. In a previous study, we showed that intravenously administered Ad35 vectors exhibited a safer profile than Ad5 vectors in cynomolgus monkeys, which ubiquitously express CD46, an Ad35 receptor, in a pattern similar to that in humans. However, the Ad35 vectors poorly transduced the organs. In this study, we examined the transduction properties of Ad35 vectors after local administration into organs of cynomolgus monkeys. The vectors transduced different types of cells depending on the organ. Hepatocytes and microglia were mainly transduced after the vectors were injected into the liver and cerebrum, respectively. Injection of the vectors into the femoral muscle resulted in the transduction of cells that appeared to be fibroblasts and/or macrophages. Conjunctival epithelial cells showed transgene expression following infusion into the vitreous body of the eyeball. Transgene expression was limited to areas around the injection points in most of the organs. In contrast, Ad35 vector-mediated transgene expression was not detected in any of the organs not injected with Ad35 vectors. These results suggest that Ad35 vectors are suitable for gene delivery by direct administration to organs.

Gene Therapy (2009) **16,** 297–302; doi:10.1038/gt.2008.154; published online 18 September 2008

Keywords: *adenovirus serotype 35 vector; local administration; nonhuman primate; CD46*

Adenoviruses (Ads) are nonenveloped, double-stranded DNA viruses with icosahedral symmetry. To date, 51 human adenovirus (Ad) serotypes have been identified and classified into six species.[1,2] Among these serotypes, Ad serotype 5 (Ad5), which belongs to species C, is the basis of almost all the Ad vectors commonly used, including those used in clinical trials. Conventional Ad5 vectors have several advantages as gene delivery vehicles. However, it is now well established that the hurdles to Ad5 vector-mediated gene therapy are the high seroprevalence to Ad5 in adults and the refractoriness of cells lacking the expression of coxsackievirus-adenovirus receptor, which is a primary receptor for Ad5, to Ad5 vectors. Pre-existing anti-Ad5 immunity significantly decreases the transduction efficiencies of Ad5 vectors. Even when an Ad5 vector-based vaccine was administered locally into muscle, pre-existing anti-Ad5 antibodies reduced its efficacy.[3,4] A lack of coxsackievirus-adenovirus receptor expression renders the cells unsusceptible to Ad5 vectors at least *in vitro*. Important target cells for gene therapy, including hematopoietic stem cells and dendritic cells, often poorly express coxsackievirus-adenovirus receptor. In addition to these drawbacks, Ad5 vectors have high hepatic tropism. Even when Ad5 vectors are locally injected into a diseased area (for example, a tumor), they are drained from the injection sites into the systemic circulation and primarily transduce hepatocytes because of their high hepatic tropism; on the other hand, efficient transduction is obtained around the injection points. When Ad vectors carry a transgene that exerts cytotoxic effects on transduced cells, Ad vector-mediated hepatic transduction leads to severe hepatotoxicity.[5–7]

In contrast, human species B Ad serotype 35 (Ad35) vectors, which our group and several others have developed,[8–11] possess attractive properties that can overcome the drawbacks of conventional Ad5 vectors. First, Ad35 vector-mediated transduction is not hampered by anti-Ad5 antibodies, because Ad35 belongs to a different species (species B) than Ad5 (species C). Second, Ad35 vectors bind to human CD46 as a receptor.

Correspondence: Dr H Mizuguchi, Laboratory of Gene Transfer and Regulation, National Institute of Biomedical Innovation, 7-6-8 Asagi, Saito, Ibaraki City, Osaka 567-0085, Japan.
E-mail: mizuguch@nibio.go.jp
[7]Current address: Research Center of Animal Life Science, Shiga University of Medical Science, Otsu City, Shiga, Japan.
Received 24 July 2008; revised 24 August 2008; accepted 24 August 2008; published online 18 September 2008

Human CD46 is expressed on almost all human cells, leading to broad tropism of Ad35 vectors in human cells, including coxsackievirus-adenovirus receptor-negative cells.[8,12] However, intravenous administration of Ad35 vectors resulted in inefficient transduction in the organs of human CD46-transgenic (CD46TG) mice and cynomolgus monkeys, which express CD46 in a pattern similar to that of humans.[13–15] These results indicate that CD46 does not successfully serve as a receptor for intravascularly injected Ad35 vectors and that Ad35 vectors are unsuitable for intravascular transduction. However, this property of Ad35 vectors would suggest a potential advantage, in that unwanted transduction would not occur in organs other than the organs targeted following direct injection of Ad35 vectors when draining from injected sites into the bloodstream. These properties suggest that Ad35 vectors would be suitable for gene transfer by local administration into the organs. In this study, we examined the transduction properties of Ad35 vectors following intraorgan administration in nonhuman primates, that is, cynomologus monkeys.

A previously constructed Ad35 vector expressing β-galactosidase (Ad35LacZ)[15] was locally administered at a dose of 1.5×10^{11} vector particles (VP) per point (high dose) or 3×10^{10} VP per point (low dose) in the following eight organs of two cynomolgus monkeys (designated no. 8 and no. 9; no. 8 received the high dose of Ad35LacZ and no. 9 received the low dose): liver, cerebrum, eyeball (vitreous body), quadriceps femoris muscle, pancreas, kidney, spleen and nasal cavity. Four days after administration, the tissues around the injection sites (approximately $40 \times 40 \times 10$ mm^3 with a central focus at the injection point) were collected and subjected to an analysis of β-galactosidase expression and histological pathology. The health condition of the monkeys was also monitored until necropsy.

Overall, both monkeys did well during the experiment. There were no apparent abnormalities in body temperature or heart rate, although no. 8, the high-dose monkey, exhibited slight reductions in blood pressure and body weight. Both monkeys apparently exhibited increased serum levels of aspartate aminotransferase and creatine phosphokinase on days 0–2 after injection. Mild decreases in hemoglobin levels and increases in levels of lactate dehydrogenase and C-reactive protein were also found in both animals. However, these changes were probably due to the operation. The levels of alanine aminotransferase, alkaline phosphatase, albumin, glucose, calcium, chloride and sodium in the serum were mostly within the normal ranges.

After the direct injection of the Ad35 vectors, the transduction profiles were assessed by immunostaining of β-galactosidase in the tissue sections; Table 1 summarizes the results. A detailed transduction profile in each organ is described below.

Liver

Direct injection of Ad35LacZ to the liver caused tissue damage around the injection site (Figures 1a and b). Infiltration of inflammatory cells, necrotic focus and regenerated bile duct epithelial cells were observed. Immunostaining of the liver sections revealed that hepatocytes were mainly transduced with Ad35LacZ in both no. 8 and no. 9 monkeys (Figures 2a and b). A higher level of β-galactosidase was expressed in the liver of no. 8 than in that of no. 9. The transduced cells were predominantly distributed around the injection point (approximately 1×1 mm^2) and were not found outside the periphery of the injection site. β-galactosidase was not expressed in the liver lobes, which were not injected with Ad35LacZ. β-galactosidase-expressing cells were mainly found on the border region between the normal and damaged areas. Direct injection of naked plasmid DNA or Ad5 vectors into mouse liver also resulted in the localized distribution of transgene-expressing cells around the injection points.[16,17] The liver would not allow dispersion of locally injected Ad vectors in the tissue.

Table 1 β-galactosidase expression in the organs following direct injection of Ad35LacZ into organs

	No. 8 (high dose)	*No. 9 (low dose)*
Liver	+++	+
Cerebrum	+++	+
Eyeball	+	−
Femoral muscle	+	+
Pancreas	−	++
Kidney	−	++
Spleen	−	−
Nasal cavity	−	−

+++, strong positive; ++, moderate positive; +, weakly positive; −, negative.

Cerebrum

Ad35LacZ was stereotaxically injected into the left frontal lobe of the cerebrum. After infusion of the high dose of Ad35LacZ, softening of the tissue, which appeared necrotic, was widely observed in the left basal ganglia (Figure 1c). Neutrophils were infiltrated into the necrotic area. In contrast, injection of a low dose of Ad35LacZ resulted in no apparent toxicity, although slight bleeding was found around the artery (Figure 1d). Transduced cells, which appeared to be microglia, were found around the softening regions of both no. 8 and no. 9 animals, although the latter had fewer transduced microglia (Figures 2c and d). There were no β-galactosidase-expressing cells in the right hemisphere of the brain, which was infused with phosphate-buffered saline buffer (data not shown).

Eye

Ad35LacZ was infused into the vitreous body for inoculation into the eyeball. The high dose induced invasion by inflammatory cells, including macrophages and neutrophils, into the ciliary body, iris and retina (Figure 1e). Necrotic changes were also found in all layers of the retina. The low dose caused similar damage to the eyeball. The high dose mediated transduction in the conjunctival epithelial cells (Figure 2e). β-galactosidase expression was not observed in other areas. After injection into the vitreous body, Ad35LacZ might be drained from it and transduce the conjunctival epithelial cells. Bora *et al.*[18] demonstrated that human CD46 was hardly expressed in eye tissues, suggesting that these tissues are refractory to Ad35 vectors. We did not find β-galactosidase expression in the eye of no. 9 animal. Phosphate-buffered saline injection did not result in

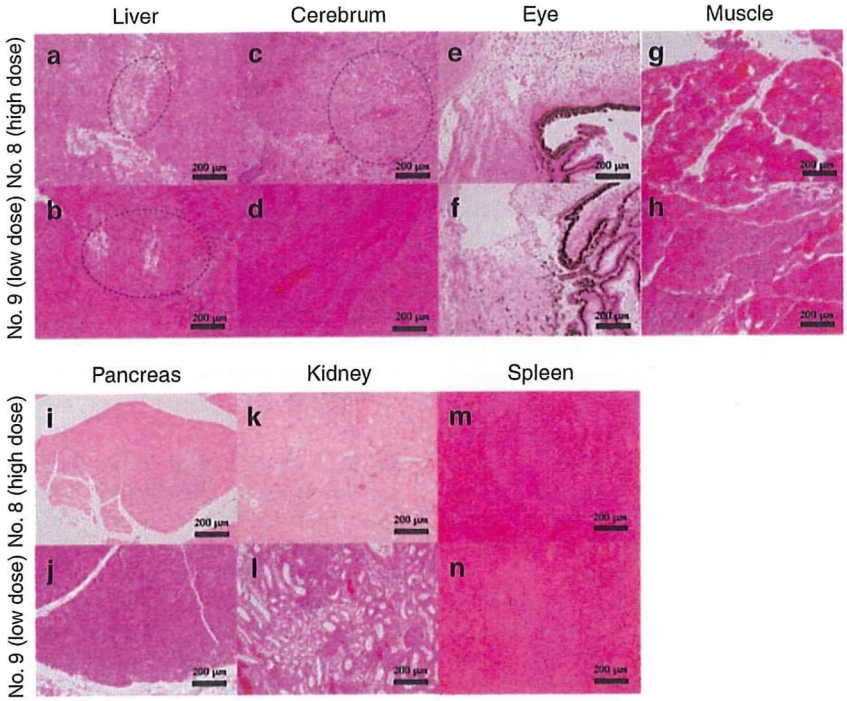

Figure 1 Tissue histology in the organs of cynomolgus monkeys 4 days after intraorgan injection of Ad35LacZ. (**a** and **b**) The liver, (**c** and **d**) cerebrum, (**e** and **f**) eyeball, (**g** and **h**) skeletal muscle, (**i** and **j**) pancreas, (**k** and **l**) kidney and (**m** and **n**) spleen. Young male cynomolgus monkeys (*Macaca fascicularis*) were housed and handled in accordance with the rules for animal care and management of the Tsukuba Primate Center and with the guiding principles for animal experiments using nonhuman primates formulated by the Primate Society of Japan. The animals (approximately 3 years of age, 1.9 and 2.2 kg) were certified free of intestinal parasites and seronegative for simian type-D retrovirus, herpesvirus B, varicella-zoster-like virus and measles virus. The protocol of the experimental procedures was approved by the Animal Welfare and Animal Care Committee of the National Institute of Biomedical Innovation (Osaka, Japan). The liver, cerebrum, eyeball, nasal cavity, pancreas, kidney, skeletal muscle and spleen of cynomolgus monkeys were each injected with Ad35LacZ suspended in 200 μl (100 μl for eyeball) of phosphate-buffered saline at a dose of 1.5×10^{11} vector particles (VP) per point (monkey no. 8) or 3×10^{10} VP per point (monkey no. 9). Four days after injection, tissue sections were hematoxylin–eosin stained by a routine method. Dotted-line circles in (**b**) and (**c**) indicate the necrotic area in the liver and the softening area in the cerebrum, respectively.

transgene expression or apparent abnormality in the eyeball (data not shown).

Femoral muscle

Severe inflammation did not occur after intramuscular injection of the high dose, although we found slight damage to the muscle fibers (Figure 1g). In contrast, the low dose induced more severe inflammation (Figure 1h). Infiltration of neutrophils and macrophages was seen in the muscle of no. 9. It is currently unclear why the low dose induced higher levels of damage. A slight difference in the injection point might affect Ad35 vector-induced inflammatory responses in the muscle. β-galactosidase expression was found only in the cells that appeared to be macrophages and/or fibroblasts located among the muscle fibers in both monkeys (Figures 2g and h). No muscle fibers expressed β-galactosidase in either monkey. It remains to be elucidated why intramuscular injection of Ad35 vectors mediated poor transduction in muscle fibers of cynomolgus monkeys. Ad35 vectors transduced the muscle following intramuscular injection in wild-type mice and in CD46TG mice.[12,14] The transduction mechanism and efficiencies of Ad35 vectors in muscle fibers might differ among species, and the muscle of nonhuman primates might be more refractory to transduction than that of rodents. Thirion *et al*.[19] demonstrated that Ad vectors would transduce human, rat and mouse primary muscle cells through different pathways. Danko *et al*.[20] reported that transgene expression levels by intramuscular injection of naked DNA were lower in dogs and nonhuman primates than in rodents. On the other hand, several studies demonstrated the utility of Ad35 vectors as vaccine vectors that express antigen by intramuscular administration in mice and nonhuman primates.[3,4] Macrophages and/or dendritic cells transduced with Ad35 vectors might play important roles in transgene-specific immune responses by intramuscular injection of Ad35 vectors.

Pancreas

Injection into the pancreas caused no severe damage to that organ in either monkey (Figures 1i and j). We did not find transduced cells in the pancreas of no. 8; in contrast, β-galactosidase was apparently expressed in exocrine acinar cells of no. 9 in the pancreatic lobules (Figures 2i and j). Chemiluminescence assay of β-galactosidase also revealed significant levels of β-galactosidase expression in the pancreas of no. 9 but not in that of no. 8 (data not shown). Wang *et al*.[21] also demonstrated that direct injection of conventional Ad vectors and adenoassociated virus vectors into murine pancreas achieved efficient transduction in acinar cells. Pancreatic acinar cells would be susceptible to Ad vectors.

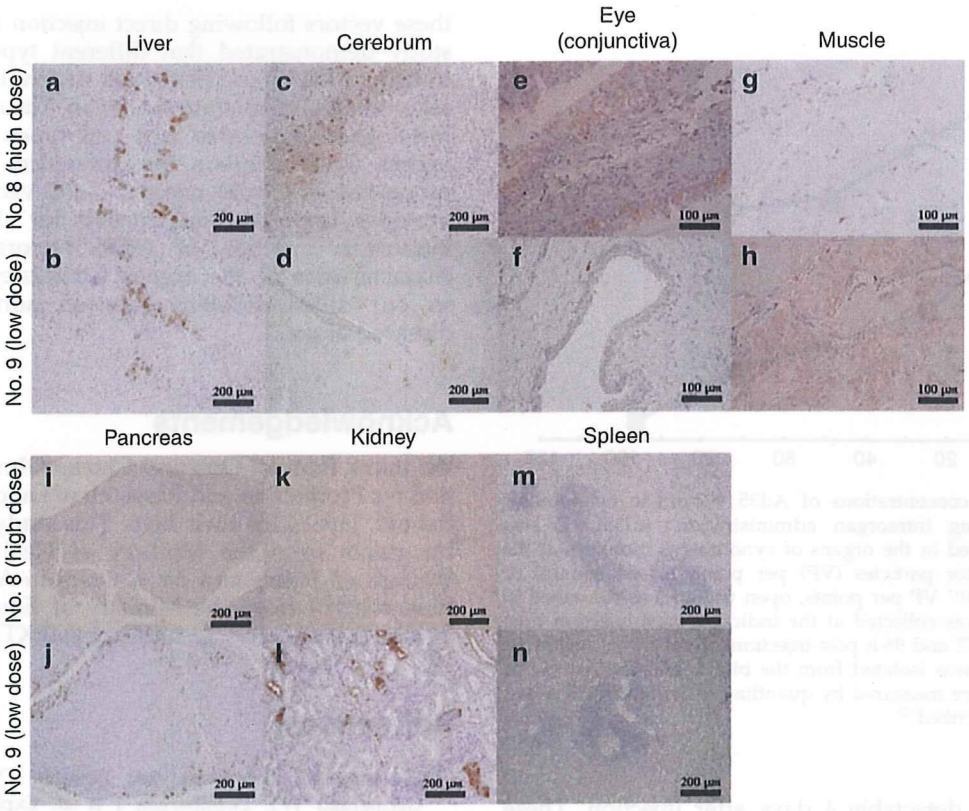

Figure 2 β-galactosidase expression in the organs of cynomolgus monkeys 4 days after intraorgan injection of Ad35LacZ. (**a** and **b**) The liver, (**c** and **d**) cerebrum, (**e** and **f**) eyeball, (**g** and **h**) skeletal muscle, (**i** and **j**) pancreas, (**k** and **l**) kidney and (**m** and **n**) spleen. Ad35LacZ was locally administered in the organs of cynomolgus monkeys at the low (3×10^{10} vector particles (VP) per point) or high dose (1.5×10^{11} VP per points) as described in Figure 1. Four days after injection, the tissues were collected for analysis of β-galactosidase expression and histological pathology. Immunostaining of β-galactosidase was performed using anti-β-galactosidase antibody (Abcam, Cambridge, UK).

Kidney

Ad35LacZ injection to the left kidney induced infiltration by inflammatory cells, including lymphocytes, into the interstitial tissue of the kidney (Figures 1k and l). The right kidney, which was injected with phosphate-buffered saline, did not exhibit β-galactosidase expression or inflammatory responses (data not shown). The high dose did not mediate β-galactosidase expression, but the low dose led to apparent transduction (Figures 2k and l). The renal tubular epithelial cells were mainly transduced with Ad35LacZ. In the kidney, compared with the other organs, transduced cells were more widely spread around the injection points. Refractoriness to the high dose and massive β-galactosidase expression by the low dose in the pancreas and kidney together form a major conundrum in this study. The differences in transduction efficiencies might be due to the slight differences in injection sites. Especially, Ad35LacZ may have been drained into the renal tubule of no. 9 following injection into the kidney, leading to efficient transduction in the renal tubule epithelial cells. Ad35 was originally identified in the kidney and causes cystitis,[22] indicating the tropism of Ad35 for renal epithelial cells.

Spleen and nasal cavity

Unexpectedly, direct injection of Ad35LacZ to the spleen did not induce inflammatory responses such as hyperplasia (Figures 1m and n). There was no β-galactosidase expression in the spleen of either monkey (Figures 2m and n). For transduction in the mucosal membrane of the nasal cavity, Ad35 vector suspensions were instilled into the nasal cavity of each monkey, but neither one showed β-galactosidase expression or cellular damage in the mucosal membrane of the nasal cavity (data not shown).

Other organs

β-galactosidase production in the lung, heart, thymus, bone marrow, lymph node, bladder and testis, which were not injected with Ad35LacZ, were examined by chemiluminescence assay. None of these organs showed detectable β-galactosidase expression (data not shown).

Next, we determined the blood concentrations of Ad35LacZ genome DNA in the blood using quantitative real-time PCR to examine whether or not Ad35LacZ locally injected to the organs was drained from the injection site into the bloodstream. The Ad35 vector DNA was detected in the blood as soon as 6 h post-injection, then gradually decreased (Figure 3). However, the blood-clearance kinetics of Ad35LacZ following intraorgan injection were slower than those following intravenous administration, which were previously reported,[23] although the total amounts of Ad35 vector doses in this study (no. 8: 1.5×10^{11} VP $\times$ 8 points; no. 9: 3×10^{10} VP $\times$ 8 points) were comparable to or lower than those in the previous study in which Ad35LacZ was intravenously infused in cynomolgus monkeys ($0.4–2 \times 10^{12}$ VP per kg, 1.88–2.96 kg).[23] Ad35 vector

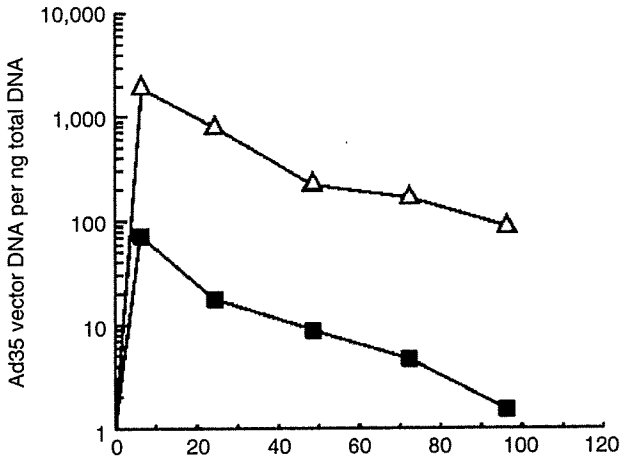

Figure 3 Blood concentrations of Ad35 vectors in cynomolgus monkeys following intraorgan administration. Ad35LacZ was locally administered in the organs of cynomolgus monkeys at the low (3×10^{10} vector particles (VP) per point, closed square) or high dose (1.5×10^{11} VP per points, open triangle) as described in Figure 1. Blood was collected at the indicated post-injection time points (6, 24, 48, 72 and 96 h post-injection). Total DNA, including Ad vector DNA, was isolated from the blood, and the Ad vector DNA contents were measured by quantitative TaqMan PCR assay, as previously described.[23]

DNA was still detectable 4 days after injection. These results suggest that Ad35 vectors or Ad35 vector DNA remaining in the injection sites might be gradually released from the injection sites and drained into the bloodstream.

Furthermore, to examine whether or not Ad35LacZ draining into the bloodstream was accumulated in the organs, we determined the Ad35 DNA contents in the portions of the liver and spleen that were away from the respective injection sites. The liver and spleen play crucial roles in the clearance of systemically injected Ad vectors. The Ad35 vector DNA was not detected in those portions of the liver in no. 9, but was detected in the portions of the liver in no. 8 and in those of the spleen in both monkeys (data not shown). These results suggest that Ad35LacZ or the Ad35 vector DNA draining into the systemic circulation would be taken up by the liver and spleen. We further assessed the Ad35 DNA contents in the lungs, heart, thymus and bone marrow, in which Ad35 vectors were not directly infused. Ad35 vector DNA was detected in the lungs and heart of no. 8 but not in those of no. 9 (data not shown). We did not detect Ad35 vector DNA in the thymus or bone marrow of either monkey. Considering that intravascularly injected Ad35 vectors did not efficiently transduce organs,[15] organs must not be transduced with Ad35LacZ, which is drained into the bloodstream and taken up by the organs.

In most cases of cancer gene therapy using Ad vectors, the vectors are administered directly to the tumor regions.[24–26] When used as vaccine vectors, on the other hand, Ad vectors are intramuscularly injected.[27,28] In addition, Ad vectors are intramyocardially injected in angiogenic gene therapy.[29,30] Thus, direct infusion of Ad vectors to organs is one of the most frequent application methods in clinical settings. However, there has been little information about the transduction properties of these vectors following direct injection into organs. This study demonstrated that different types of cells were transduced with Ad35 vectors depending on the organ after direct infusion into the organ. The differences in the histological structures and cell types comprising the organs would explain the differences in transduction properties of locally injected Ad35 vectors. This study provides important information for clinical study by intraorgan injection of Ad35 vectors, although the characteristics of the organs (structure, cell types and so on) differ different between normal tissue and diseased areas.

Acknowledgements

We thank Fumiko Ono and Chieko Ohno (The Corporation for Production and Research of Laboratory Primates, Ibaraki, Japan) for their help. This study was supported by grants from the Ministry of Health, Labour, and Welfare of Japan and by a Grant-in-Aid for Scientific Research (B) from the Ministry of Education, Culture, Sports, Science, and Technology (MEXT) of Japan.

References

1 Havenga MJ, Lemckert AA, Ophorst OJ, van Meijer M, Germeraad WT, Grimbergen J *et al.* Exploiting the natural diversity in adenovirus tropism for therapy and prevention of disease. *J Virol* 2002; **76**: 4612–4620.
2 De Jong JC, Wermenbol AG, Verweij-Uijterwaal MW, Slaterus KW, Wertheim-Van Dillen P, Van Doornum GJ *et al.* Adenoviruses from human immunodeficiency virus-infected individuals, including two strains that represent new candidate serotypes Ad50 and Ad51 of species B1 and D, respectively. *J Clin Microbiol* 1999; **37**: 3940–3945.
3 Lemckert AA, Sumida SM, Holterman L, Vogels R, Truitt DM, Lynch DM *et al.* Immunogenicity of heterologous prime-boost regimens involving recombinant adenovirus serotype 11 (Ad11) and Ad35 vaccine vectors in the presence of anti-ad5 immunity. *J Virol* 2005; **79**: 9694–9701.
4 Nanda A, Lynch DM, Goudsmit J, Lemckert AA, Ewald BA, Sumida SM *et al.* Immunogenicity of recombinant fiber-chimeric adenovirus serotype 35 vector-based vaccines in mice and rhesus monkeys. *J Virol* 2005; **79**: 14161–14168.
5 Mizuguchi H, Hayakawa T. Enhanced antitumor effect and reduced vector dissemination with fiber-modified adenovirus vectors expressing herpes simplex virus thymidine kinase. *Cancer Gene Ther* 2002; **9**: 236–242.
6 Okada Y, Okada N, Mizuguchi H, Hayakawa T, Mayumi T, Mizuno N. An investigation of adverse effects caused by the injection of high-dose TNFalpha-expressing adenovirus vector into established murine melanoma. *Gene Therapy* 2003; **10**: 700–705.
7 Suzuki T, Sakurai F, Nakamura S, Kouyama E, Kawabata K, Kondoh M *et al.* miR-122a-regulated expression of a suicide gene prevents hepatotoxicity without disturbing the antitumor effects in suicide gene therapy. *Mol Ther* 2008, (in press).
8 Sakurai F, Mizuguchi H, Hayakawa T. Efficient gene transfer into human CD34+ cells by an adenovirus type 35 vector. *Gene Therapy* 2003; **10**: 1041–1048.
9 Vogels R, Zuijdgeest D, van Rijnsoever R, Hartkoorn E, Damen I, de Bethune MP *et al.* Replication-deficient human adenovirus type 35 vectors for gene transfer and vaccination: efficient human cell infection and bypass of preexisting adenovirus immunity. *J Virol* 2003; **77**: 8263–8271.

10 Gao W, Robbins PD, Gambotto A. Human adenovirus type 35: nucleotide sequence and vector development. *Gene Therapy* 2003; **10**: 1941–1949.
11 Seshidhar Reddy P, Ganesh S, Limbach MP, Brann T, Pinkstaff A, Kaloss M *et al*. Development of adenovirus serotype 35 as a gene transfer vector. *Virology* 2003; **311**: 384–393.
12 Sakurai F, Mizuguchi H, Yamaguchi T, Hayakawa T. Characterization of *in vitro* and *in vivo* gene transfer properties of adenovirus serotype 35 vector. *Mol Ther* 2003; **8**: 813–821.
13 Sakurai F, Kawabata K, Koizumi N, Inoue N, Okabe M, Yamaguchi T *et al*. Adenovirus serotype 35 vector-mediated transduction into human CD46-transgenic mice. *Gene Therapy* 2006; **13**: 1118–1126.
14 Verhaagh S, de Jong E, Goudsmit J, Lecollinet S, Gillissen G, de Vries M *et al*. Human CD46-transgenic mice in studies involving replication-incompetent adenoviral type 35 vectors. *J Gen Virol* 2006; **87**: 255–265.
15 Sakurai F, Nakamura S, Akitomo K, Shibata H, Terao K, Kawabata K *et al*. Transduction properties of adenovirus serotype 35 vectors after intravenous administration into nonhuman primates. *Mol Ther* 2008; **16**: 726–733.
16 Sakai M, Nishikawa M, Thanaketpaisarn O, Yamashita F, Hashida M. Hepatocyte-targeted gene transfer by combination of vascularly delivered plasmid DNA and *in vivo* electroporation. *Gene Therapy* 2005; **12**: 607–616.
17 Crettaz J, Berraondo P, Mauleon I, Ochoa L, Shankar V, Barajas M *et al*. Intrahepatic injection of adenovirus reduces inflammation and increases gene transfer and therapeutic effect in mice. *Hepatology* 2006; **44**: 623–632.
18 Bora NS, Gobleman CL, Atkinson JP, Pepose JS, Kaplan HJ. Differential expression of the complement regulatory proteins in the human eye. *Invest Ophthalmol Vis Sci* 1993; **34**: 3579–3584.
19 Thirion C, Lochmuller H, Ruzsics Z, Boelhauve M, Konig C, Thedieck C *et al*. Adenovirus vectors based on human adenovirus type 19a have high potential for human muscle-directed gene therapy. *Hum Gene Ther* 2006; **17**: 193–205.
20 Danko I, Williams P, Herweijer H, Zhang G, Latendresse JS, Bock I *et al*. High expression of naked plasmid DNA in muscles of young rodents. *Hum Mol Genet* 1997; **6**: 1435–1443.
21 Wang AY, Peng PD, Ehrhardt A, Storm TA, Kay MA. Comparison of adenoviral and adeno-associated viral vectors for pancreatic gene delivery *in vivo*. *Hum Gene Ther* 2004; **15**: 405–413.
22 Hierholzer JC. Adenoviruses in the immunocompromised host. *Clin Microbiol Rev* 1992; **5**: 262–274.
23 Sakurai F, Nakamura S, Akitomo K, Shibata H, Terao K, Hayakawa T *et al*. Transduction properties of adenovirus serotype 35 vectors after intravenous administration in non-human primates. *Mol Ther* 2008; **16**: 726–733.
24 Shirakawa T, Terao S, Hinata N, Tanaka K, Takenaka A, Hara I *et al*. Long-term outcome of phase I/II clinical trial of Ad-OC-TK/VAL gene therapy for hormone-refractory metastatic prostate cancer. *Hum Gene Ther* 2007; **18**: 1225–1232.
25 Shimada H, Matsubara H, Shiratori T, Shimizu T, Miyazaki S, Okazumi S *et al*. Phase I/II adenoviral p53 gene therapy for chemoradiation resistant advanced esophageal squamous cell carcinoma. *Cancer Sci* 2006; **97**: 554–561.
26 Tong AW, Nemunaitis J, Su D, Zhang Y, Cunningham C, Senzer N *et al*. Intratumoral injection of INGN 241, a nonreplicating adenovector expressing the melanoma-differentiation associated gene-7 (mda-7/IL24): biologic outcome in advanced cancer patients. *Mol Ther* 2005; **11**: 160–172.
27 Catanzaro AT, Koup RA, Roederer M, Bailer RT, Enama ME, Moodie Z *et al*. Phase 1 safety and immunogenicity evaluation of a multiclade HIV-1 candidate vaccine delivered by a replication-defective recombinant adenovirus vector. *J Infect Dis* 2006; **194**: 1638–1649.
28 Rosenberg SA, Zhai Y, Yang JC, Schwartzentruber DJ, Hwu P, Marincola FM *et al*. Immunizing patients with metastatic melanoma using recombinant adenoviruses encoding MART-1 or gp100 melanoma antigens. *J Natl Cancer Inst* 1998; **90**: 1894–1900.
29 Stewart DJ, Hilton JD, Arnold JM, Gregoire J, Rivard A, Archer SL *et al*. Angiogenic gene therapy in patients with nonrevascularizable ischemic heart disease: a phase 2 randomized, controlled trial of AdVEGF(121) (AdVEGF121) versus maximum medical treatment. *Gene Therapy* 2006; **13**: 1503–1511.
30 Rosengart TK, Lee LY, Patel SR, Kligfield PD, Okin PM, Hackett NR *et al*. Six-month assessment of a phase I trial of angiogenic gene therapy for the treatment of coronary artery disease using direct intramyocardial administration of an adenovirus vector expressing the VEGF121 cDNA. *Ann Surg* 1999; **230**: 466–470; discussion 470–472.

Correspondence

BOTULINUM TOXIN FOR DIABETIC NEUROPATHIC PAIN: A RANDOMIZED DOUBLE-BLIND CROSSOVER TRIAL

BOTULINUM TOXIN FOR NEUROPATHIC PAIN?

To the Editor: We are skeptical of the benefits of botulinum toxin type A (BoNT/A) in treating neuropathic pain.[1] We also believe that Apfel's[2] accompanying editorial was too positive regarding this study involving only 18 patients.

Sleep problems and quality of life scores have nothing in common with results of the visual analog scale (VAS) and these are our patients' major concerns. In addition, the pattern of injections is not related to the areas where our patients complain about pain, including the toes and balls of the feet. Furthermore, data have shown that injection sites followed the pain.[3,4]

The study would have benefited by having independent funding rather than relying on the largess of Allergan for the BoNT/A. BoNT/A has proven indications, but the drive to expand them is industry-driven and is reminiscent of the marketing strategy of Neurontin. Given its cost and mode of use, larger studies funded by unrelated sources should be pursued.

Josh Torgovnick, Edward Arsura, Nitin K. Sethi, New York, NY

Disclosure: The authors report no disclosures.

Reply from the Authors: We thank Torgovnick et al. for their comments and would like to address their concerns.

First, we surveyed the quality of sleep and life because they are both affected by neuropathic pain. Most patients with diabetic neuropathy complain about sleep interference caused by pain. Sleep disturbance in turn increases the pain sensation and decreases quality of life.[5] We wanted to explore neuropathic pain in life quality among diabetic patients.

Second, the effects of BoNT/A on foot sensation were unclear before this study. If BoNT/A impaired all sensory modalities, including proprioception over toes and balls of the feet, participants might have gait disturbance including sensory ataxia. This possibility concerned our IRB when we submitted our proposal. In addition, intradermal injection was not easy due to the skin thickness of these regions. We agree with Torgovnick et al. that toes and balls of the feet or "following the pain" method should be the first consideration in subsequent trials.[3,4]

Finally, Allergan was not involved during the complete course of this double-blinded study. We searched for novel resolutions of patient problems based on scientific knowledge and academic interest. To create new indications of BoNT/A for neuropathic pain, larger clinical trials are needed regardless of funding sources.

Chaur-Jong Hu, Rey-Yue Yuan, Jau-Jiuan Sheu, Taipei, Taiwan

Disclosure: The authors report no disclosures.

Reply from the Editorialist: Although Torgovnick et al. comment that my editorial was too positive regarding this small study,[1] I acknowledged this limitation and highlighted the need to conduct larger, carefully designed, multicenter, clinical trials.[2]

The optimism of the editorial was based on the fact that the results of 2 independent studies were largely in agreement.[1,3] This does not constitute proof of efficacy, but should encourage others to conduct larger, appropriately designed clinical trials.

The authors further imply that the source of funding for this study may have biased the results. That is always a concern with private funding of any research. However, without such funding, vital clinical and basic science research would not secure sponsorship. Extensive regulatory oversight of pharmaceutical industry research provides strict—if not stricter—quality control and transparency than the academic setting, where peer review is largely the only check and balance on researchers struggling to "publish or perish."

Stuart C. Apfel, West Hempstead, NY

Disclosure: Dr. Apfel, in his capacity as founder and principal of Parallax Clinical Research, has served as a paid consultant for Tolerx Inc., Acambis Pharmaceuticals, Asubio Pharmaceuticals, Cara Pharmaceuticals, Eisai Pharmaceuticals, ITI Pharmaceuticals, and Elite

Pharmaceuticals, and has served as Chief Medical Officer for and received stock options from Elite Pharmaceuticals.

1. Yuan RY, Sheu JJ, Yu JM, et al. Botulinum toxin for diabetic neuropathic pain: a randomized double-blind crossover trial. Neurology 2009;72:1473–1478.
2. Apfel SC. Botulinum toxin for neuropathic pain? Neurology 2009;72:1456–1457.
3. Ranoux D, Attal N, Morain F, Bouhassira D. Botulinum toxin type A induces direct analgesic effects in chronic neuropathic pain. Ann Neurol 2008;64:274–284.
4. Piovesan EJ, Teive HG, Kowacs PA, Della Coletta MV, Werneck LC, Silberstein SD. An open study of botulinum A toxin treatment of trigeminal neuralgia. Neurology 2005;65:1306–1308.
5. Parish JM. Sleep-related problems in common medical conditions. Chest 2009;135:563–572.

SILENT ISCHEMIC INFARCTS ARE ASSOCIATED WITH HEMORRHAGE BURDEN IN CEREBRAL AMYLOID ANGIOPATHY

To the Editor: We read the article by Kimberly et al.,[1] who showed that small subacute infarcts were detected on MRI in patients with advanced cerebral amyloid angiopathy (CAA).

The authors retrospectively detected 17 DWI-hyperintense lesions in 78 subjects with probable CAA, but found no lesions in 55 subjects with Alzheimer disease (AD) or mild cognitive impairment. An association was not found between leukoaraiosis and the 17 ischemic lesions including 4 lesions found in the cortical gray matter.

The distribution of microvascular lesions and the absence of their relation to leukoaraiosis is notable since CAA is usually observed in the subarachnoid and intracortical vessels, frequently accompanied by leukoaraiosis. In AD brains, cerebral microbleeds have shown occipital predominance and correspondence to parieto-occipital leukoaraiosis.[2]

In addition, microinfarcts are typically found in the cortical borderzone with occipital predominance in subjects with dementia.[3] We further reported that microinfarcts were frequently detected in the cerebral cortices of postmortem AD brains, whereas they were rarely found in subcortical vascular dementia.[4] These cortical microinfarcts were distributed predominantly in proximity to amyloid β (A β)-deposited vessels with severe morphologic changes. In terms of arterial supply and cortical layers, most were distributed in the posterior superficial borderzone, and mainly in the cortical layers 2–3.

Predilection of microinfarcts in the borderzone may be attributed to insufficient Aβ clearance in these regions, because pulsation of the vessels plays an important role in perivascular lymphatic drainage of Aβ.[5] Taken together, differences may exist in regional distribution and relation to leukoaraiosis between CAA-related microvascular lesions with or without AD.

Yoko Okamoto, Masafumi Ihara, Hidekazu Tomimoto, Kyoto City, Japan

Disclosure: The authors report no disclosures.

Reply from the Authors: Dr. Okamoto et al. comment on their observation that microinfarcts are common in brains with AD, with predilection for the borderzone regions of the brain and for occurring near vascular amyloid deposits. The relation between these lesions and the microinfarcts observed in association with advanced CAA is intriguing.

Pathologic specimens of patients with CAA have not supported any specific vascular distribution for these lesions,[6-8] but have generally not provided quantitative analysis of stroke burden within each region of the brain. Similarly, our cross-sectional MRI-based study did not demonstrate a borderzone predominance. This question is difficult to assess, however, since our analysis is limited by the small number of events and difficulty defining the precise location of the borderzone.

We note that our control AD group excluded patients with microbleeds, thus minimizing the severity of CAA in this group. Our MRI data may therefore underestimate the incidence of microinfarcts in AD.

W. Taylor Kimberly, Steven M. Greenberg, Boston, MA

Disclosure: Dr. Greenberg serves on the scientific advisory board for Hoffman-LaRoche and is funded by NIH RO1 AG026484 and K24 NS056207. Dr. Kimberly reports no disclosures.

1. Kimberly WT, Gilson A, Rost NS, et al. Silent ischemic infarcts are associated with hemorrhage burden in cerebral amyloid angiopathy. Neurology 2009;72:1230–1235.
2. Pettersen JA, Sathiyamoorthy G, Gao FQ, et al. Microbleed topography, leukoaraiosis, and cognition in probable Alzheimer disease from the Sunnybrook dementia study. Arch Neurol 2008;65:790–795.
3. Kövari E, Gold G, Herrmann FR, et al. Cortical microinfarcts and demyelination affect cognition in cases at high risk for dementia. Neurology 2007;68:927–931.
4. Okamoto Y, Ihara M, Fujita Y, et al. Cortical microinfarcts in Alzheimer's disease and subcortical vascular dementia. NeuroReport 2009;20:990–996.
5. Weller RO, Djuanda E, Yow HY, Carare RO. Lymphatic drainage of the brain and the pathophysiology of neurological disease. Acta Neuropathol 2009;117:1–14.
6. Okazaki H, Reagan TJ, Campbell RJ. Clinicopathologic studies of primary cerebral amyloid angiopathy. Mayo Clin Proc 1979;54:22–31.
7. Cadavid D, Mena H, Koeller K, Frommelt RA. Cerebral beta amyloid angiopathy is a risk factor for cerebral ischemic infarction: a case control study in human brain biopsies. J Neuropathol Exp Neurol 2000;59:768–773.
8. Haglund M, Passant U, Sjobeck M, Ghebremedhin E, Englund E. Cerebral amyloid angiopathy and cortical microinfarcts as putative substrates of vascular dementia. Int J Geriatr Psychiatry 2006;21:681–687.

VASCULAR SMOOTH MUSCLE CELL DYSFUNCTION IN PATIENTS WITH MIGRAINE

To the Editor: The article by Napoli et al.[1] describing experimental techniques to quantify vascular endothelial reactivity illuminates the presence of arterial endothelial acetylcholine receptors which are known to be coupled to the NO vasodilatory pathway.

The endothelial cholinergic receptors are presumably associated with vascular cholinergic nerve terminals arising from nervi vasorum present in the arterial tunica adventitia. Such cholinergic vascular nerve terminals have been demonstrated in skin biopsy specimens using stains for acetylcholinesterase. Cholinergic nerve terminals are the target of botulinum toxin, raising the possibility that cholinergic denervation of the scalp arteries may underlie the benefit of botulinum toxin injections in the treatment of migraine.

Typical injection sites used for treatment of migraine in the areas of the temporalis, frontalis, and occipitalis muscles are close to the temporal, supraorbital, and occipital arteries. Abundant data exist describing the role of vasodilation of the extracranial scalp arteries in a subset of patients with migraine. Does cholinergic denervation of the scalp arteries reduce vasodilation and thereby ameliorate migraine? The findings of Napoli et al. suggest that this may not be the case as responsiveness to intravascular acetylcholine is reduced in patients with migraine.

The hypothesis that cholinergic denervation of the scalp arteries may underlie the benefit of cranial botulinum toxin injections in the treatment of migraine should be explored.

William N. Devor, MD, San Diego, CA

Disclosure: Dr. Devor received an honorarium from Plaza Research and administers botulinum toxin for treatment of headache in a nonprofit setting.

Reply from the Authors: We thank Dr. Devor for his interest in our article on vascular reactivity in patients with migraine.[1] Endothelial dysfunction and abnormal vascular reactivity are involved in the onset and progression of atherosclerosis and subsequently the increased risk of cardiovascular diseases.

Given the increased risk of cardiovascular events associated with migraine, we aimed to explore the reactivity of both endothelial and vascular smooth muscle cells (VSMCs) in patients with migraine in the headache-free state. We found that in patients with migraine studied in the interictal period, endothelial function is normal and a clear defect in the VSMCs response emerges. In human vessels, acetylcholine vasodilatory response is due to the stimulation of specific receptors located on the surface of the endothelial cells which in turn activate nitric oxide synthase in order to produce nitric oxide (NO).

Once released, NO triggers vasodilation by stimulating cGMP production in the VSMCs. In our data, the response to the intraarterial infusion of acetylcholine is reduced in patients with migraine. However, this reduction is not due to a defect in the ability of acetylcholine to induce NO production and release by the endothelial cells, but rather to a severe impairment of VSMCs to respond to NO stimulation. This is demonstrated because we detected a normal release of NO during acetylcholine infusion by the endothelial cells. In addition, there was an impaired vasodilation during the infusion of sodium nitroprusside (a NO donor) in patients with migraine due to the insufficient response to NO by the VSMCs.

Therefore, acetylcholine response by the endothelial cells in patients with migraine during the interictal period is normal. Since we were interested in the mechanisms of cardiovascular risk, we studied vascular reactivity in the brachial artery as a well-established model of coronary vascular reactivity. However, the relationship between peripheral vascular reactivity and cerebral circulation is still unclear.

Since we studied vascular reactivity in the headache-free period, the vascular mechanisms underlying the migraine attack in both peripheral and cerebral circulation cannot be clarified by our study. The possibility arises that vascular reactivity can be different during the migraine attack.

Raffaele Napoli, L. Saccà, Naples, Italy

Disclosure: Drs. Napoli and Saccà received compensation for a study from Pfizer Italia.

1. Napoli R, Guardasole V, Zarra E, et al. Vascular smooth muscle cell dysfunction in patients with migraine. Neurology 2009;72:2111–2114.

Cortical microinfarcts in Alzheimer's disease and subcortical vascular dementia

Yoko Okamoto[a], Masafumi Ihara[a], Youshi Fujita[a], Hidefumi Ito[a], Ryosuke Takahashi[a] and Hidekazu Tomimoto[b]

Cortical microinfarcts are reported in Alzheimer's disease, but not in subcortical vascular dementia; the disease specificity of cortical microinfarcts therefore remains unclear. The distribution of cortical microinfarcts in Alzheimer's disease ($n=8$) and subcortical vascular dementia ($n=6$) was analyzed. Cortical microinfarcts were frequently detected in Alzheimer's disease, whereas they were rarely observed in subcortical vascular dementia. In Alzheimer's disease, cortical microinfarcts were present predominantly in the occipital lobe, the area of predilection for amyloid angiopathy, and also in the vascular borderzone. Cortical microinfarcts were invariably located very close to amyloid β-deposited vessels with intercellular adhesion molecule-1 expression. These results indicate that cortical microinfarcts are caused by the pathomechanism related to Alzheimer's disease, most likely to amyloid angiopathy. *NeuroReport* **20:990–996**

NeuroReport 2009, 20:990–996

Keywords: Alzheimer's disease, amyloid angiopathy, cortical microinfarct, subcortical vascular dementia

[a]Department of Neurology, Graduate School of Medicine, Kyoto University, Kyoto and [b]Department of Neurology, Graduate School of Medicine, Mie University, Mie, Japan

Correspondence to Dr Yoko Okamoto, Department of Neurology, Graduate School of Medicine, Kyoto University, 54 Kawaharacho, Shogoin, Sakyo-ku, Kyoto 606-8507, Japan
Tel/fax: +81 75 751 3766; e-mail: yoko416@kuhp.kyoto-u.ac.jp

Received 14 March 2009 **accepted** 17 April 2009

Introduction

Recently, an increasing body of evidence has indicated that vascular risk factors, such as hypertension and diabetes mellitus have a pivotal role in the pathogenesis of Alzheimer's disease [1]. Accordingly, the Nun study has shown that the risk of dementia increases more than 20 times in Alzheimer's disease, if the patients have foci of cerebral infarctions [2]. Cortical microinfarcts were predominantly observed in the vascular borderzone of Alzheimer's disease brains [3], and were found to be a strong determinant for dementia, in a manner comparable with the neuropathological hallmarks that determine Alzheimer's disease [4–6].

The pathoetiology and disease specificity of cortical microinfarcts remain elusive. It is unclear whether cortical microinfarcts are present exclusively in Alzheimer's disease brains, or are associated with hypertensive small-vessel disease. In this study, we compared the distribution of cortical microinfarcts in Alzheimer's disease and subcortical vascular dementia, focusing especially on their spatial correlation with amyloid angiopathy.

Materials and methods

Human tissue

Two hundred and seventy autopsied brains were obtained from the Kyoto University Hospital and its affiliated hospitals from 1988 to 2007 through a process approved by an institutional research committee. Among the 270 brains, there included 13 Alzheimer's disease brains and six subcortical vascular dementia brains. We excluded five Alzheimer's disease brains because of concomitant macroscopic cerebral infarctions. We examined the remaining eight Alzheimer's disease brains (mean ± SEM: 79 ± 4 years old) and six subcortical vascular dementia brains (mean ± SEM: 77 ± 5 years old). These Alzheimer's disease and subcortical vascular dementia patients met the diagnostic criteria for dementia (*Diagnostic and Statistical Manual of Mental Disorders*, fourth edition) [7]. The diagnosis of Alzheimer's disease was based on the Consortium to Establish a Registry for Alzheimer's Disease diagnostic neuropathologic criteria [8], and the Braak and Braak neuropathological staging of Alzheimer-related changes [9].

The diagnosis of subcortical vascular dementia was made clinicopathologically to meet the criteria of: (i) the presence of bilateral diffuse subcortical lesions, (ii) lacunar infarctions in the perforator territory, (iii) arteriolosclerosis, such as fibrohyalinosis and fibrinoid necrosis, and (iv) the absence of cortical infarctions, and the clinical criteria outlined by Bennett *et al.* [10]. Cases with significant pathological hallmarks of Alzheimer's disease (senile plaque Braak stage ≥ B, neurofibrillary tangle Braak stage ≥ II [9]) were excluded.

Immunohistochemical staining

Tissue blocks obtained from the frontal, temporal, parietal, and occipital lobes were embedded in paraffin. Histological assessment was carried out with hematoxylin and eosin (H&E), Klüver–Barrera, and modified Bielschowsky staining. The rest of the blocks were used for immunohistochemistry as described earlier [11]. The

0959-4965 © 2009 Wolters Kluwer Health | Lippincott Williams & Wilkins DOI: 10.1097/WNR.0b013e32832d2e6a

primary antibodies consisted of: rabbit anti-glial fibrillary acidic protein (GFAP) (diluted 1:200; Dako, Glostrup, Denmark), mouse anti-human cluster of differentiation 68 (CD68) (1:100; Dako), mouse anti-amyloid β-protein (1:100; Novocastra, Newcastle, UK), and mouse anti-intercellular adhesion molecule-1 (ICAM-1) (1:100; Santa Cruz Biotechnology, Santa Cruz, California, USA). For IgG, horseradish peroxidase-labeled anti-human IgG (1:50; Dako), and for actin, rhodamin-labeled phalloidin (1:200; Invitrogen Corporation, Carlsbad, California, USA) were used.

Image analysis

Images of the histological slides were captured with a digital camera (CAMEDIA C-7070; Olympus, Tokyo, Japan) and scanned (Canon, CanoScan N1220U; Canon Inc., Tokyo, Japan). In each slide, cortical areas were outlined and the corresponding numbers of pixels were counted using the ImageJ software package (National Institute of Health; Bethesda, Maryland, USA).

Definition and count of cortical microinfarcts

Cortical microinfarcts had not been defined earlier, and were therefore determined according to the following criteria: a cortical lesion that was not noticeable until examined microscopically and accompanied by a group of astrocyte or microglia/macrophage proliferation. Histological changes likely to be expanded Virchow–Robin spaces, microabscesses, or cortical laminar necrosis were excluded.

After measuring the number of microinfarcts and the cortical area in each specimen, we calculated the number of cortical microinfarcts (per cm^2) infiltrated by numerous GFAP-positive astrocytes or CD68-positive microglia/macrophages.

The cerebral cortex was divided into five regions according to the arterial supply of anterior, middle, and posterior cerebral arteries, and their two borderzones (anterior-middle and middle-posterior), based on the text atlas [12]. The borderzone was defined as the area within 3 cm apart from the proposed borderline [12], and the number of microinfarcts was calculated similarly as stated above. The distribution of microinfarcts was further studied in terms of their topographic relationships to the cortical layers and the cerebral convolutions. Briefly, microinfarcts were classified into those distributed in layers 1–3 or 4–6, or alternatively, into those located in the crown part, the sulcal part, or the depth of the sulcal part.

The topographical relationship between Aβ-positive vessels and microinfarcts was also assessed. Microinfarcts were judged to adjoin Aβ-deposited vessels, if they were localized within 1 mm of these vessels. Senile plaque load was assessed with modified Bielschowsky staining in the region containing each microinfarct. The severity of senile plaque load was divided into four groups: those with none, sparse, moderate, and frequent in accordance with the Consortium to Establish a Registry for Alzheimer's Disease criteria [8].

Statistical analysis

Data were statistically analyzed using one-way analysis of variance, followed by Bonferroni's post-hoc test (Statview version 5.0, SAS Institute, Cary, North Carolina, USA).

Results

All microinfarcts detected in H&E stains were invariably accompanied by GFAP-positive astroglia. The mean diameter of the microinfarcts was approximately 200 μm (range 100–500). Cortical microinfarcts were found in all

Fig. 1

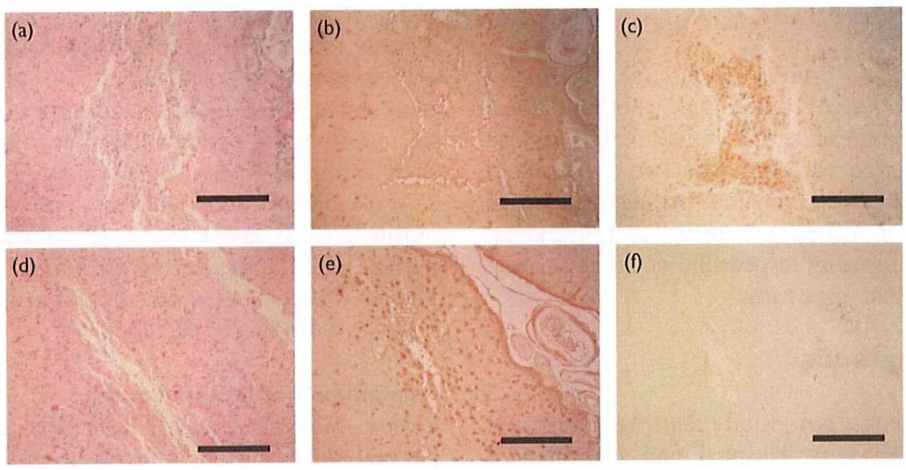

Photomicrographs of cortical microinfarcts with (a–c) and without microglial activation (d–f). The upper panels (a–c) and lower panels (d–f) are adjacent sections. Hematoxylin and eosin staining (a, d), immunohistochemistry for glial fibrillary acidic protein (GFAP; b, e), and cluster of differentiation 68 (CD68; c, f). Bars indicate 300 μm.

eight Alzheimer's disease brains and one of the six subcortical vascular dementia brains, and were classified into two groups: microinfarcts with or without infiltration of CD68-positive microglia/macrophages (Fig. 1). The lesions that had been infiltrated both by astroglia and microglia/macrophages were considered to be relatively recent infarcts. The lesions with astrogliosis, but without CD68-positive microglia/macrophages, were considered to be older. This is because both astroglia and microglia/macrophages are activated in the acute stage of cerebral infarction, but macrophages regress within several months.

In H&E stains, lesions accompanied by erythrocytes or hemosiderin depositions were excluded. Furthermore, Perls–Stieda staining was added to search for iron deposits and IgG immunohistochemistry for serum protein extravasation, so that microhemorrhagic lesions could be ruled out. Only a minority (3%) of cortical microlesions were accompanied by iron deposits or IgG-positive astroglia, indicating that most microlesions are not caused by hemorrhagic mechanisms (compare Fig. 2a and c, and Fig. 2b and d).

Fig. 2

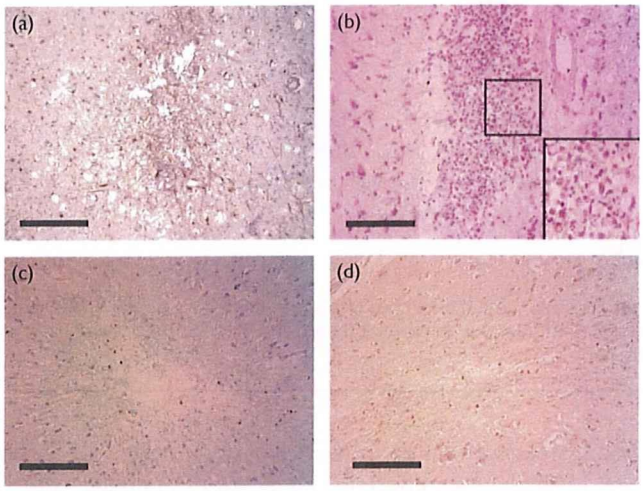

Photomicrographs of cortical microinfarcts (CMIs) with immunohistochemical staining for IgG (a, c) and Perls–Stieda staining to detect iron depositions (b, d). Note IgG-positive astroglia (a) or iron deposits (b, inset). (c) and (d) show CMIs without IgG-positive glia or iron deposits, respectively. Bars in (a) indicate 250 μm, and in (b–d) 200 μm.

The numerical densities of cortical microinfarcts with GFAP-positive astroglia in Alzheimer's disease were 0.45, 0.14, 0.43, and 1.08 (per cm^2) in the frontal, temporal, parietal, and occipital lobes, respectively. The densities of cortical microinfarcts with CD68-positive microglia/macrophages were 0.11, 0.04, 0.00, and 0.44, respectively, in each lobe (Table 1 and Fig. 3a). In contrast, in subcortical vascular dementia, the numerical densities of cortical microinfarcts with GFAP-positive astroglia were 0.058, 0.015, 0, and 0, respectively, in each lobe (per cm^2) (Table 1). Thus, cortical microinfarcts were frequent in Alzheimer's disease, but were rarely found in subcortical vascular dementia.

In Alzheimer's disease, there was a marginally significant increase of microinfarcts with GFAP-positive astroglia in the occipital lobe compared with the temporal lobe ($P = 0.0511$), whereas there was only an increased tendency compared with the other lobes (occipital vs. frontal, $P = 0.1709$; frontal vs. parietal, $P = 0.9775$; frontal vs. temporal, $P = 0.5118$). In terms of the arterial supply, the numerical densities of cortical microinfarcts with GFAP-positive astroglia were 0.40, 0.19, 0.28, 0.66, and 1.47 (per cm^2) in Alzheimer's disease in the anterior, middle, and posterior cerebral arteries, anterior-middle cerebral arterial boderzone, and middle-posterior cerebral arterial borderzone, respectively (Table 1 and Fig. 3b). Most of the microinfarcts were distributed in the superficial borderzones. In terms of cortical layers, the number of microinfarcts with GFAP-positive astroglia was significantly different between the superficial and the deep

Table 1 The distribution of microinfarcts in different cortical regions

	Layer		Convolution[a]			AA	Lobe (per 1 cm^2)[b]				Vascular territory (per 1 cm^2)[c]					SP[d]			
Number of cortical microinfarcts	1–3	4–6	C	S	D	(+)	F	T	P	O	A	A/M	M	M/P	P	N	S	M	F
AD ($n=8$)																			
HE	40	9	25	1	23	26/49	0.28	0.08	0.20	0.44	0.16	0.37	0.07	0.82	0.00	0	13	19	17
GFAP	73	19	42	8	42	46/92	0.45	0.14	0.43	1.08	0.40	0.66	0.19	1.47	0.28	0	25	42	25
CD68	15	5	10	0	10	16/20	0.11	0.04	0.00	0.44	0.07	0.21	0.02	0.68	0.00	0	9	11	0
SVD ($n=6$)																			
HE	4	0	1	1	2	0/4 (0%)	0.043	0.015	0	0	0	0.029	0	0	0.028	4	0	0	0
GFAP	5	0	2	1	2	0/5 (0%)	0.058	0.015	0	0	0	0.048	0	0	0.028	5	0	0	0
CD68	4	0	1	1	2	0/4(0%)	0.043	0.015	0	0	0	0.029	0	0	0.028	4	0	0	0

AA, amyloid angiopathy; +, the rate of AA-positive cortical microinfarcts; AD, Alzheimer's disease; HE, hematoxylin and eosin; GFAP, glial fibrillary acidic protein; CD68, cluster of differentiation 68; SVD, subcortical vascular dementia.
[a]C, crown part; D, depth; S, sulcal part.
[b]F, frontal; O, occipital; P, parietal; T, temporal.
[c]A, A/M, M, M/P, P denotes anterior, middle, and posterior cerebral arteries, and their borderzones, respectively.
[d]F, frequent; M, moderate; N, none; S, sparse; SP, senile plaque.

Fig. 3

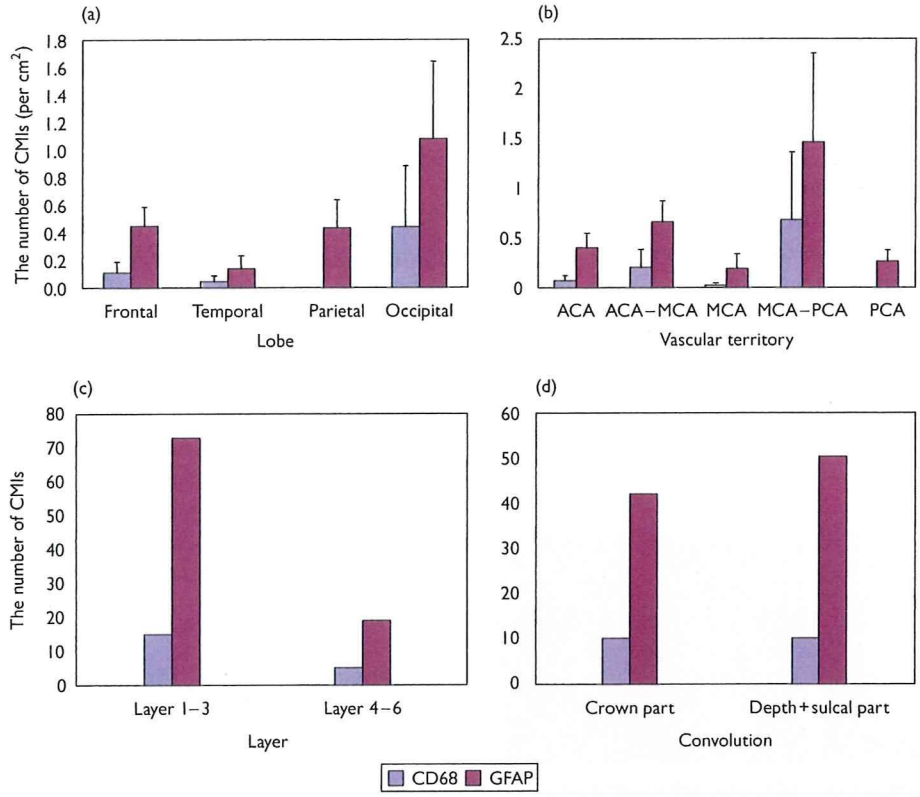

The density of cortical microinfarcts (CMIs/cm^2) in each lobe (a) and vascular territories (b), and the number of CMIs in cortical layers (c) and inside the cerebral convolutions (d). ACA, MCA, PCA, A/M, M/P denote anterior, middle, and posterior cerebral arteries, and their borderzones, respectively. CD68, cluster of differentiation 68; GFAP, glial fibrillary acidic protein.

layers of the Alzheimer's disease brains (73 vs. 19, respectively, $P = 0.0080$ by one-way analysis of variance) (Table 1 and Fig. 3c). However, no trends were found in terms of spatial distribution within the cerebral convolution (Table 1 and Fig. 3d).

Aβ-immunoreactive vessels were observed in six cases of the eight Alzheimer's disease brains, but not in six subcortical vascular dementia brains. Interestingly, Aβ deposition was predominantly in the vessels apposed to microinfarcts (Fig. 4). Such vessels were tortuous or double-barrel in shape. Half of the cortical microinfarcts with GFAP-positive astroglia (46 out of the 92) were localized less than 1 mm apart from Aβ-positive vessels. ICAM-1 was preferentially expressed in the endothelial cells and vessel walls surrounding microinfarcts (Fig. 5a and b). Double labeling for ICAM-1 and actin showed that the vessels around microinfarcts commonly express ICAM-1 (Fig. 5c–e). The number of microinfarcts was not associated with senile plaque burden (Table 2).

Discussion

Sporadic cerebral amyloid angiopathy (CAA) is a state in which Aβ deposits in the cerebral vessels, and has been strongly related with the presence of dementia [13]. Thal *et al.* [14,15] have reported two types of sporadic CAA: capillary CAA and classical CAA. In capillary CAA, Aβ deposits are present within capillaries; whereas in classical CAA, Aβ initially deposits at the outer basement membrane of the leptomeningeal and cortical arteries, and then within their smooth muscle layer [14,15]. As both the capillary and classical CAA pathologies were present in most of the brains with Alzheimer's disease, further investigation is required to know which of the two pathologies underlies cortical microinfarcts.

CAA is dormant during lifetime, whereas it leads to major cerebral hemorrhage (approximately 5–20%) or infarct in a subset of elderly patients [16]. As a facilitating factor, the ApoE ε2 and ε4 alleles are related to a higher risk for CAA or CAA-associated hemorrhage [14–16]. In this study, the ApoE genotype was not assessed; therefore, it remains unknown whether there is a relationship between ApoE genotype and cortical microinfarcts in Alzheimer's disease.

The occipital lobe is most commonly and severely affected in CAA [14–16]. In this study, GFAP-positive

Fig. 4

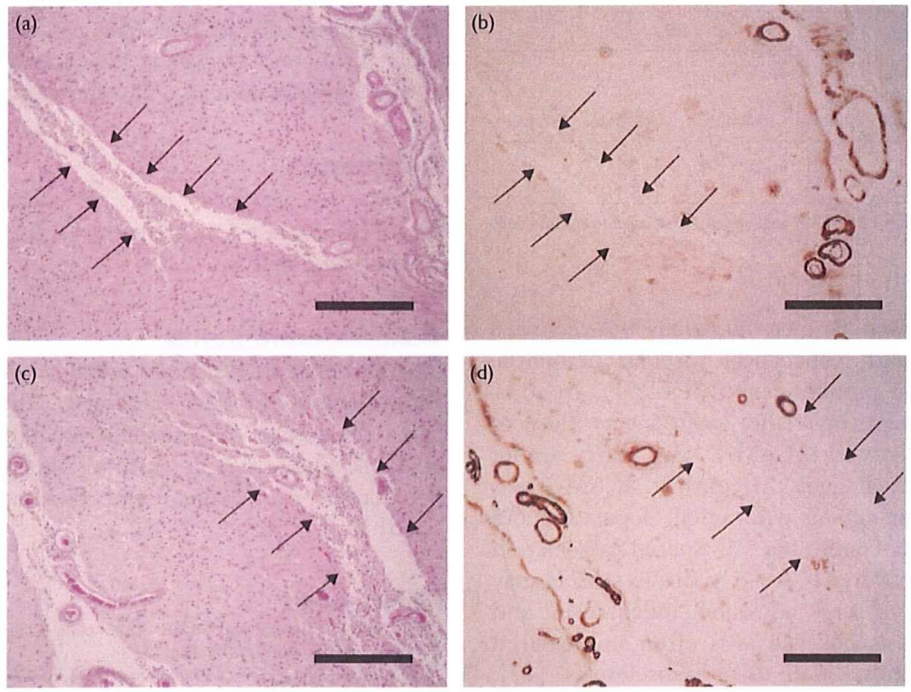

Photomicrographs of cortical microinfarcts with hematoxylin and eosin staining (a, c) and immunohistochemistry for Aβ (b, d). The upper panels (a, b) and lower panels (c, d) are adjacent sections. Arrows indicate microinfarcts. Bars in (a–d) indicate 250 μm.

Fig. 5

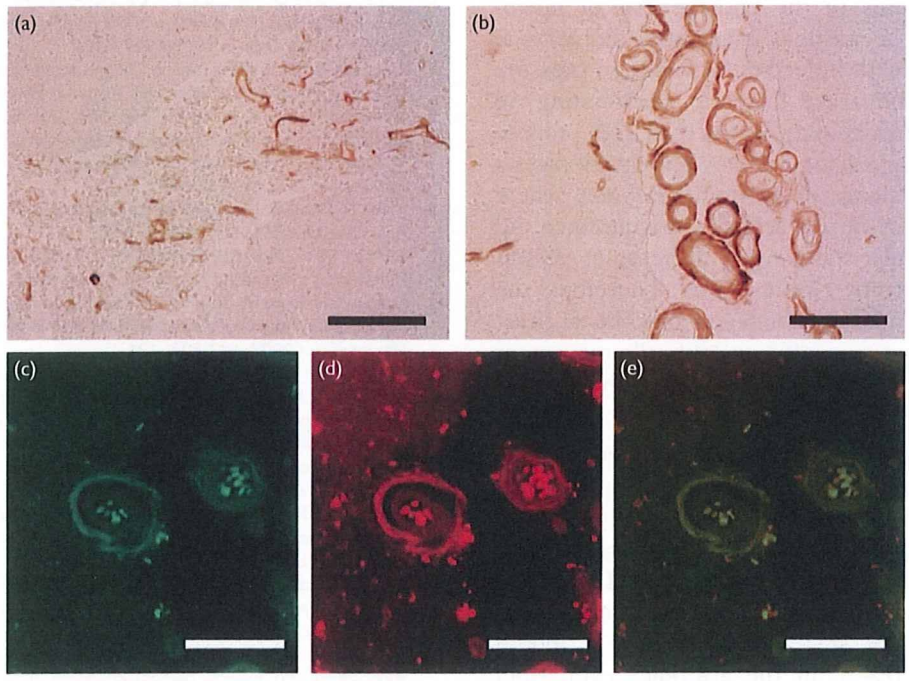

Photomicrographs of immunohistochemistry for intercellular adhesion molecule-1 (ICAM-1) (a–c), actin (d), and double labeling for ICAM-1 and actin (e). Bars in (a), (c–e) indicate 100 μm, and in (b) 200 μm.

Table 2 The number of GFAP-positive or CD68-positive cortical microinfarcts and their associations with senile plaque burden

		SP			
Cortical microinfarcts	Total number of cortical microinfarcts	None	Sparse	Moderate	Frequent
GFAP-positive	92	0	25	42	25
CD68-positive	20	0	9	11	0

CD68, cluster of differentiation 68; GFAP, glial fibrillary acidic protein; SP, senile plaque.

cortical microinfarcts were far more numerous in Alzheimer's disease compared with subcortical vascular dementia, and showed occipital predominance (Table 1). In addition, microinfarcts were invariably located very close to Aβ-deposited vessels with ICAM-1 expression and/or severe morphological changes. In contrast, ICAM-1 was rarely detected in the vessels without Aβ deposition and those in quiescent conditions. A spatial association between microinfarcts and ICAM-1 positive vessels may indicate activation of cell adhesion mechanism and subsequent thrombosis because it is often upregulated in inflammatory states, such as atherosclerosis [17]. In correspondence with these findings, occipital predominance has also been revealed in the distribution of microbleeds, which are also attributed to CAA [18].

Microinfarcts were distributed not only in the occipital lobe, but also in the superficial borderzone, in accordance with the earlier study [3]. Predilection of microinfarcts in the borderzone territory suggests that hypoperfusion in these areas contributes to the pathogenesis of microinfarcts in addition to amyloid angiopathy. Borderzone territory is irrigated with a decreased perfusion pressure [19] and this may be a key factor in ameliorating Aβ deposition [20,21]. Intriguingly, Weller *et al.* [22] propose that lymphatic drainage along capillary and artery plays a significant role in drainage of Aβ from the brain, where pulsatile movement of vessels acts as a driving force. Aβ clearance along vascular walls might decrease as vessels stiffen with age, thereby causing CAA. Therefore, the observed predilection of microinfarcts may be at least partially explained by the insufficient pulsatile movement and augmented Aβ deposition in the borderzone area.

In an earlier study, this group has reported cortical microvascular changes in Alzheimer's disease and their absence in subcortical vascular dementia [11]. The capillary densities in Alzheimer's disease were significantly decreased with various morphological changes, such as tearing or narrowing of the cortical microvessels. Furthermore, Stopa *et al.* [23] have reported that smooth muscle actin is decreased in the arterioles even from the early stages of Alzheimer's disease. In contrast to the medullary arteries, which consistently show arteriosclerotic changes in the white matter, small vessel changes were rarely found in the cerebral cortices of subcortical vascular dementia. Different patterns of small vessel changes in topographical distribution may consequently explain the clear distinction between Alzheimer's disease and subcortical vascular dementia in terms of cortical microinfarcts.

Conclusion

Cortical microinfarcts may be caused by the pathomechanism related to Alzheimer's disease, most likely to amyloid angiopathy.

Acknowledgements

The authors express their cordial gratitude to Dr Ahmad Khundakar for critical reading of the manuscript and Miss Nakabayashi for excellent technical assistance. This study is supported, in part, by the Mochida Memorial Foundation for Medical and Pharmaceutical Research (to M.I.).

References

1 Kalaria RN. Similarities between Alzheimer's disease and vascular dementia. *J Neurol Sci* 2002; **203–204**:29–34.
2 Snowdon DA, Greiner LH, Mortimer JA, Riley KP, Greiner PA, Markesbery WR. Brain infarction and the clinical expression of Alzheimer disease. The Nun Study. *JAMA* 1997; **277**:813–817.
3 Suter OC, Sunthorn T, Kraftsik R, Straubel J, Darekar P, Khalili K, *et al.* Cerebral hypoperfusion generates cortical watershed microinfarcts in Alzheimer disease. *Stroke* 2002; **33**:1986–1992.
4 White L, Petrovitch H, Hardman J, Nelson J, Davis DG, Ross GW, *et al.* Cerebrovascular pathology and dementia in autopsied Honolulu-Asia Aging Study participants. *Ann NY Acad Sci* 2002; **977**:9–23.
5 Kövari E, Gold G, Herrmann FR, Canuto A, Hof PR, Michel JP, *et al.* Cortical microinfarcts and demyelination significantly affect cognition in brain aging. *Stroke* 2004; **35**:410–414.
6 Kövari E, Gold G, Herrmann FR, Canuto A, Hof PR, Bouras C, *et al.* Cortical microinfarcts and demyelination affect cognition in cases at high risk for dementia. *Neurology* 2007; **68**:927–931.
7 American Psychiatric Association. *Diagnostic and Statistical Manual of Mental Disorders.* 4th ed. Washington DC: American Psychiatric Association; 1994.
8 Mirra SS, Heyman A, McKeel D, Sumi SM, Crain BJ, Brownlee LM, *et al.* The Consortium to Establish a Registry for Alzheimer's Disease (CERAD). Part II. Standardization of the neuropathologic assessment of Alzheimer's disease. *Neurology* 1991; **41**:479–486.
9 Braak H, Braak E. Neuropathological staging of Alzheimer-related changes. *Acta Neuropathol* 1991; **82**:239–259.
10 Bennett DA, Wilson RS, Gilley DW, Fox JH. Clinical diagnosis of Binswanger's disease. *J Neurol Neurosurg Psychiatry* 1990; **53**:961–965.
11 Kitaguchi H, Ihara M, Saiki H, Takahashi R, Tomimoto H. Capillary beds are decreased in Alzheimer's disease, but not in Binswanger's disease. *Neurosci Lett* 2007; **417**:128–131.
12 Kretschmann HJ, Weinrich W. *Neuroanatomy and cranial computed tomography.* New York, USA: Thieme-Stratton Corp.; 1986.
13 Neuropathology Group of the Medical Research Council Cognitive Function and Aging Study. Pathological correlates of late-onset dementia in a multicentre, community-based population in England and Wales. *Lancet* 2001; **357**:169–175.
14 Thal DR, Griffin W ST, de Vos R AI, Ghebremedhin E. Cerebral amyloid angiopathy and its relationship to Alzheimer's disease. *Acta Neuropathol* 2008; **115**:599–609.
15 Thal DR, Ghebremedhin E, Rüb U, Yamaguchi H, Tredici KD, Braak H. Two types of sporadic cerebral amyloid angiopathy. *J Neuropathol Exp Neurol* 2002; **61**:282–293.
16 Attems J. Sporadic cerebral amyloid angiopathy: pathology, clinical implications, and possible pathomechanisms. *Acta Neuropathol* 2005; **110**:345–359.
17 Braun M, Pietsch P, Schrör K, Braumann G, Felix SB. Cellular adhesion molecules on vascular smooth muscle cells. *Cardiovascular Research* 1999; **41**:395–401.

18 Pettersen JA, Sathiyamoorthy G, Gao FQ, Szilagyi G, Nadkarni NK, St George-Hyslop P, *et al.* Microbleed topography, leukoaraiosis, and cognition in probable Alzheimer disease from the Sunnybrook Dementia Study. *Arch Neurol* 2008; **65**:790–795.
19 Torvik A. The pathogenesis of watershed infarcts in the brain. *Stroke* 1984; **15**:221–223.
20 Ihara M, Kalaria RN. Amyloid-β and synaptic activity in mice and men. *Neuroreport* 2007; **18**:1205–1206.
21 Román GC, Kalaria RN. Vascular determinants of cholinergic deficits in Alzheimer disease and vascular dementia. *Neurobiol Aging* 2006; **27**:1769–1785.
22 Weller RO, Djuanda E, Yow HY, Carare RO. Lymphatic drainage of the brain and the pathophysiology of neurological disease. *Acta Neuropathol* 2009; **117**:1–14.
23 Stopa EG, Butala P, Salloway S, Johanson CE, Gonzalez L, Tavares R, *et al.* Cerebral cortical arteriolar angiopathy, vascular beta-amyloid, smooth muscle actin, Braak stage, and APOE genotype. *Stroke* 2008; **39**: 814–821.

BRAIN RESEARCH 1294 (2009) 202–210

available at www.sciencedirect.com

ScienceDirect

www.elsevier.com/locate/brainres

BRAIN RESEARCH

Research Report

Chronic cerebral hypoperfusion accelerates amyloid β deposition in APPSwInd transgenic mice

Hiroshi Kitaguchi[a], *Hidekazu Tomimoto*[a,*], *Masafumi Ihara*[a], *Masunari Shibata*[a], *Kengo Uemura*[a], *Rajesch N. Kalaria*[d], *Takeshi Kihara*[c], *Megumi Asada-Utsugi*[b], *Ayae Kinoshita*[b], *Ryosuke Takahashi*[a]

[a]*Department of Neurology, Kyoto University, Sakyo-ku, Kyoto, 606-8504, Japan*
[b]*School of Health Sciences, Graduate School of Medicine, Kyoto University, Sakyo-ku, Kyoto, 606-8504, Japan*
[c]*Department of Neuroscience for Drug Discovery, Graduate School of Pharmaceutical Sciences, Kyoto University, Sakyo-ku, Kyoto, 606-8501, Japan*
[d]*Institute for Health and Ageing, University of Newcastle upon Tyne, Newcastle General Hospital, Westgate Road, Newcastle-upon-Tyne, NE4 6BE, UK*

ARTICLE INFO

Article history:
Accepted 22 July 2009
Available online 30 July 2009

Keywords:
Cerebral ischemia
Amyloid β
Amyloid precursor protein
Transgenic mouse

ABSTRACT

Chronic cerebral ischemia may accelerate clinicopathological changes in Alzheimer's disease. We have examined whether chronic cerebral hypoperfusion accelerates amyloid β deposition in amyloid protein precursor transgenic (APP-Tg) mouse. At 5, 8, and 11 months of age, C57Bl/6J male mice overexpressing a mutant form of the human APP bearing the both Swedish (K670N/M671L) and the Indiana (V717F) mutations (APPSwInd) and their litterrmates were subjected to either sham operation or bilateral carotid artery stenosis (BCAS) using microcoils with an internal diameter of 0.18 mm (short-period group). One month after the sham operation or BCAS, these animals were examined by immunohistochemistry for glial fibrillary acidic protein, amyloid β_{1-40} ($A\beta_{1-40}$), amyloid β_{1-42} ($A\beta_{1-42}$), as well as Western blotting and filter assay for Aβ. Another batch of the littermates of APPSwInd mice were subjected to either sham operation or BCAS at 3 months and were examined in the same manner after survival for 9 months (long-period group). In the BCAS-treated group, the white matter was rarefied and astroglia was proliferated. Amyloid β_{1-40} immunoreactivity was found in a few axons in the white matter after BCAS, whereas $A\beta_{1-42}$ was accumulated in the scattered cortical neurons and the axons at ages of 6 months and thereafter in the short- and long-period groups. In the neuropil, both $A\beta_{1-40}$ and $A\beta_{1-42}$ were deposited in the sham-operated and BCAS-treated mice at ages of 9 and 12 months. There were no differences between the short-period group at ages of 12 months and the long-period group. Filter assay showed an increase of Aβ fibrils in the extracellular enriched fraction. Taken together, chronic cerebral hypoperfusion increased Aβ fibrils and induced Aβ deposition in the intracellular compartment and, therefore, may accelerate the pathological changes of Alzheimer's disease.

* *Corresponding author.* Present address: Department of Neurology, Graduate School of Medicine, Mie University, 2-174 Edobashi, Tsu, 514-8507, Japan. Fax: +81 59 231 5107.
E-mail address: tomimoto@clin.medic.mie-u.ac.jp (H. Tomimoto).

0006-8993/$ – see front matter © 2009 Elsevier B.V. All rights reserved.
doi:10.1016/j.brainres.2009.07.078